DTU Library

DTU

AlGaAs-On-Insulator Nanowire with 750 nm FWM Bandwidth, -9 dB CW Conversion Efficiency, and Ultrafast Operation Enabling Record Tbaud Wavelength Conversion

Pu, Minhao; Ottaviano, Luisa; Semenova, Elizaveta; Vukovic, Dragana; Oxenløwe, Leif Katsuo; Yvind, Kresten

AlGaAs-On-Insulator Nanowire with 750 nm FWM Bandwidth, -9 dB CW Conversion Efficiency, and Ultrafast Operation Enabling Record Tbaud Wavelength Conversion

M. Pu, H. Hu, L. Ottaviano, E. Semenova, D. Vukovic, L. K. Oxenløwe, and K. Yvind

DTU Fotonik, Department of Photonics Engineering, Technical University of Denmark, Ørsteds Plads 343, DK-2800 Lyngby, Denmark
mipu@fotonik.dtu.dk

Abstract: We present an AlGaAs-on-insulator platform for integrated nonlinear photonics. We demonstrate the highest reported conversion efficiency/length/pump-power, ultra-broadband four-wave mixing, and first-ever wavelength conversion of 1.28-Tbaud serial data signals in a 3-mm long dispersion-engineered AlGaAs nano-waveguide.

OCIS codes: (190.4380) Four-wave mixing; (190.4390) Integrated optics; (130.7405) Wavelength conversion devices.

1. Introduction

The search for an ideal nonlinear platform for optical signal processing has been going on for decades. Such a material would display both a high conversion efficiency, broad bandwidth range and preferably be suitable for photonic integration. Many impressive demonstrations have been made with different materials, but none has been able to simultaneously fulfill all these requirements. Highly nonlinear fibers (HNLFs) yield the highest reported conversion efficiencies accumulated through tens of meters of fiber [1]. Silicon (Si) nano-waveguides yield the highest reported four-wave mixing bandwidths [2], but suffer from two-photon absorption (TPA) reducing the obtainable conversion efficiency. Other integrated platforms for nonlinear photonics include amorphous silicon [3], Hydex glass [4], silicon nitride [5], chalcogenide [6], or semiconductors with active carrier injection or removal with electronic circuitry like Si-PIN structures [7] or semiconductor optical amplifiers (SOAs) [8]. In the all-passive cases a lot of progress has been made, but stable broad-bandwidth and highly efficient continuous wave (CW) conversion or indeed powerful system demonstrations with continuous data is still not attainable. In the biased cases, The SOAs have relatively slow recovery times due to carrier dynamics, while the Si-PiN structures have demonstrated record-high conversion at 1550 nm, albeit for a limited bandwidth [9]. Recently the prospect of using III-V nano-waveguides, such as InGaP [10] and AlGaAs [11] for pure Kerr-effect operation has emerged. This nonlinear platform offers as high an effective nonlinearity as silicon but without two-photon absorption (TPA) in the telecom wavelength range. For AlGaAs, a high nonlinear coefficient (n_2) of ~1.43×10^{-17} m^{2}W^{-1} has been reported [12], with a bandgap tailored by adjusting the Al concentration during epitaxial growth to avoid TPA around 1550 nm. Nonlinear parametric processes like four-wave mixing (FWM) have been demonstrated in deep-etched AlGaAs waveguides [11-13]. However, the low vertical index contrast mandates a challenging deep etching process, which limits more advanced designs. In addition, high index contrast is desired for enhancing light confinement.

In this paper, we demonstrate record performance of an AlGaAs-on-insulator (AlGaAsOI) platform, where a thin AlGaAs layer on top of an insulator layer resides on a semiconductor substrate. A highly efficient FWM with a CW conversion efficiency of -8.7 dB is demonstrated in a 3-mm long nano-waveguide with only 145 mW pump power. This results in a record-high TPA-free figure of merit (FOM) for ridge waveguides of 0.71 W^{-2}mm^{-2}. In addition, an ultra-broad FWM conversion bandwidth (>750 nm) is obtained. As a sufficiently challenging system demonstration, which has never been attainable before, we show that this platform has the sufficient bandwidth, conversion efficiency and speed to facilitate the world's first 1.28 Tbaud wavelength conversion. We demonstrate all-optical wavelength conversion (AOWC) of a 1.28 Tbit/s serial, single-polarization, differential phase-shift keying (DPSK) data signal. The operation is validated by bit-error rate (BER) measurements, and the result is completely error-free employing an FEC-module for all 128 optical time division multiplexing (OTDM) tributaries, resulting in the highest successful signal processing speed achieved with any nonlinear platform to date.

2. AlGaAsOI nano-waveguide

Fig. 1(a) shows the schematic layout of an AlGaAsOI nano-waveguide. A thin Al$_{0.15}$Ga$_{0.85}$As film is fabricated on an insulator layer (SiO$_2$) through wafer bonding and substrate removal. The nano-waveguide is defined using electron-beam lithography and dry etching. Fig. 1(b) shows the scanning electron microscopy (SEM) picture of a fabricated AlGaAsOI nano-waveguide before depositing the SiO$_2$ layer. Compared to deep-etched AlGaAs waveguides [11-13], the AlGaAsOI nano-waveguides provide much larger index difference (~1.8) and thus much stronger light confinement as shown for the TE mode in Fig. 1(a), which significantly enhances the effective nonlinearity. The nano-waveguide under test is inverse tapered to 120 nm at both facets of the chip for efficient fiber-to-chip coupling. We
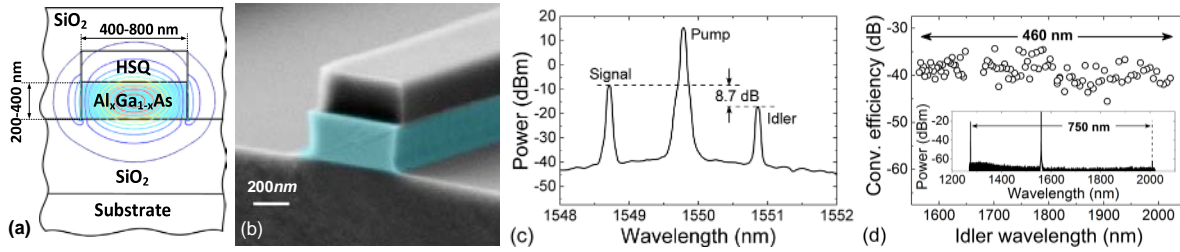
Fig.1 (a) Schematic drawing of an AlGaAsOI nano-waveguide. (b) SEM picture of a fabricated AlGaAsOI nano-waveguide (denoted by the artificial blue color). (c) Measured FWM spectrum with 145 mW pump power. (d) Measured conversion efficiency with 20 mW pump power as a function of idler wavelength (pump wavelength: 1560 nm. Inset: Measured FWM spectrum for ultra-broadband conversion.

performed a FWM measurement using two CW signals in such a waveguide. Fig. 1(c) shows the measured FWM spectrum at the output of the waveguide. A conversion efficiency of -8.7 dB is obtained using 145 mW pump power in a device of only 3 mm length. Compared with deep-etched AlGaAs waveguides [11-13], the AlGaAsOI nano-waveguide offers the highest FOM (0.71 $W^{-2}mm^{-2}$) as defined in [13]. In addition, the stronger light confinement in AlGaAsOI nano-waveguides also enable a very efficient dispersion engineering, which allows for ultra-broadband FWM operation. Fig. 1(d) shows the measured output conversion efficiency for a 3-mm long device (cross-section: 290×630 nm^2) with 20 mW pump power as a function of idler wavelength. It is seen that there is no conversion efficiency drop for idler wavelengths over a 460 nm range. The measurable bandwidth is only limited by available tunable laser sources. The conversion bandwidth is thus larger than 750 nm (1270-2020 nm) (inset of Fig. 1(d)), which easily allows for wavelength conversion of ultra-fast signals over a large wavelength range.

3. Experimental setup for system experiment and results

The experimental setup for the wavelength conversion of a 1.28-Tbit/s serial return-to-zero (RZ) DPSK signal is shown in Fig. 2 (Left). In the 1.28-Tbit/s transmitter, the 10-GHz pulse train is generated from a mode-locked laser and then compressed by self-phase modulation [14]. The generated short pulses are DPSK modulated by a 10-Gbit/s FEC (6.6% overhead) coded data pattern in a Mach-Zehnder modulator (MZM) [15]. The modulated 10-Gbit/s DPSK signal is multiplexed in time to 1.28 Tbit/s using a passive fiber-delay multiplexer (MUX ×128). The generated 1.28-Tbit/s RZ-DPSK signal at 1550 nm is launched into the AlGaAsOI nano-waveguide together with a CW pump at 1568 nm through a WDM coupler. Both pump and signal waves are aligned to TE polarization of the AlGaAsOI nano-waveguide. The input pump power is kept at 35.5 mW to ensure good fiber-to-chip alignment stability.
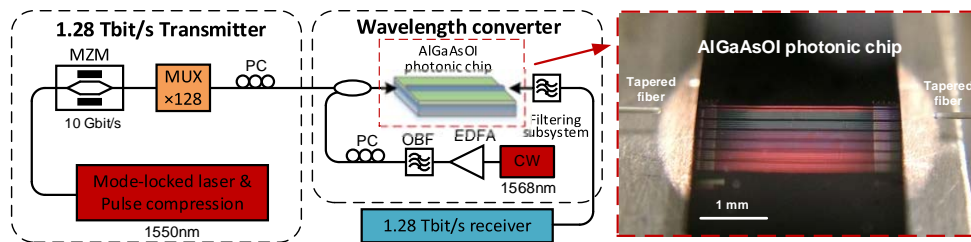

Fig.2 (Left) Experimental setup for AOWC of a 1.28 Tbit/s DPSK data signal. (Right) Photograph of the AlGaAsOI photonic chip.

Fig. 3(a) shows the optical spectra at the input (grey curve) and the output (black curve) of the nano-waveguide. The wavelength converted 1.28-Tbit/s RZ-DPSK signal at 1586 nm is extracted from the pump and signal using a filtering subsystem, consisting of optical bandpass filters and an EDFA in between (see Fig. 3(b)). The wavelength-converted signal is characterized in the time domain by measuring autocorrelation traces (Fig. 3(c) and (d)). The pulse width (FWHM: 340 fs) of the wavelength converted data pulses is almost unchanged compared to the input data pulses (FWHM: 350 fs) as a benefit of an abundant conversion bandwidth. The converted 1.28-Tbit/s OTDM signal is received by a 1.28-Tbit/s time-domain optical Fourier transformation (TD-OFT) based OTDM receiver [16], and the demultiplexed 10 Gbit/s channels are detected by a 10 Gbit/s DPSK receiver, and finally decoded by a FEC decoder. The performance of the converted signal is evaluated by error counting before and after FEC decoding. Fig. 3(e) shows the BER measurements before the FEC decoding for both the back-to-back 1.28 Tbit/s signal and the converted 1.28 Tbit/s signal. The inset of Fig. 3(e) shows the 10 Gbit/s demultiplexed and demodulated eye diagram from the 1.28 Tbit/s wavelength converted RZ-DPSK signal. The wavelength-converted 1.28-Tbit/s RZ-DPSK signal achieves a BER well below the FEC limit of 3×10^{-3} for all 128 tributaries as shown in Fig. 3(f) (upper). The wavelength conversion experiment is performed at moderate pump power (minimum to achieve proper conversion), which limits
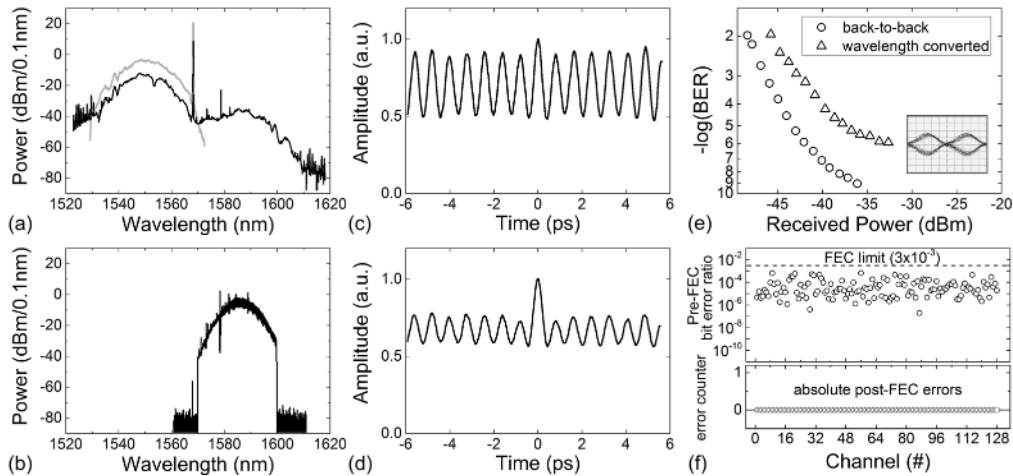
Fig.3 (a) Spectra at the input and output of the AlGaAsOI nano-waveguide. (b) Spectrum of the converted signal after filtering and amplification. (c, d) Autocorrelation trace of the input signal (c) and the output converted signal (d). (e) BER measurements for the 1.28 Tbit/s back-to-back and wavelength converted signal. Inset: eye diagram of a 10 Gbit/s demultiplexed channel from the 1.28 Tbit/s converted signal. (f) BER for all the 128 OTDM tributaries of the 1.28 Tbit/s converted signal.

the conversion efficiency to -23 dB. Therefore, the optical signal-to-noise ratio (OSNR) of the signal degrades after the conversion, resulting in an error floor at BER~10^{-5}. The error floor could be lowered if the conversion efficiency is increased by simply increasing the pump power. We also measure the absolute post-FEC errors (Fig. 3(f) (lower)). The FEC module properly corrects the errors to yield zero errors for all 128 demultiplexed 10 Gbit/s channels of the wavelength-converted signal. This corresponds to a post-FEC error-free performance at a net data rate of 1.2 Tbit/s.

4. Conclusion

We have demonstrated an AlGaAsOI platform for integrated nonlinear photonics. We demonstrate a high conversion efficiency of -8.7 dB at 145 mW pump power level in a 3-mm long device, resulting in a record TPA-free FOM for ridge waveguides of 0.71 $W^{-2}mm^{-2}$. Also achieved is an ultra-broad FWM conversion bandwidth of 750 nm. We also demonstrate on-chip AOWC of a 1.28-Tbit/s line-rate (1.2-Tbit/s net rate) RZ-DPSK signal based on FWM. This is the first demonstration of on-chip AOWC of a data signal at a speed beyond Terabit/s and indeed the fastest in any platform. The results show great potential for the proposed nonlinear platform for ultrafast optical signal processing.

Acknowledgements

References

[1] T. Torounidis et al, "Fiber-optical parametric amplifier with 70-dB gain," *IEEE Photon. Technol. Lett.* **18** 1194 (2006).
[2] A. C. Turner-Foster et al, "Frequency conversion over two-thirds of an octave in silicon nanowaveguides," *Opt. Express* **20** 6488 (2012).
[3] C. Grillet et al, "Amorphous silicon nanowires combining high nonlinearity, FOM and optical stability," *Opt. Express* **20** 22609 (2012).
[4] D.J. Moss et al, "New CMOS-compatible platforms based on silicon-nitride and Hydex glass for nonlinear optics," *Nat. Photon.* **7** 597 (2014).
[5] Y. Okawachi et al, "Octave-spanning frequency comb generation in a silicon nitride chip," *Opt. Lett.* **36** 3398 (2011).
[6] F. Luan et al, "Dispersion engineered As₂S₃ planar waveguides for broadband four-wave mixing based wavelength conversion of 40 Gb/s signals," *Opt. Express* **17** 3514 (2009).
[7] A. Gajda et al, "Highly efficient CW parametric conversion at 1550nm in SOI waveguides by reverse biased p-i-n junction," *Opt. Express* **20** 13100 (2012).
[8] M. Matsuura, "320 Gbit/s wavelength conversion using four-wave mixing in quantum-dot semiconductor optical amplifier," *Opt. Lett.* **36** 2910 (2011).
[9] F.Da Ros et al, "Phase regeneration of DPSK signals in a silicon waveguide with reverse-biased p-i-n junction," *Opt. Express* **22** 5029 (2014).
[10] U.D. Dave et al, "Nonlinear properties of dispersion engineered InGaP photonic wire waveguides in the telecommunication wavelength range," *Opt. Express* **23** 4650 (2015).
[11] J. J. Wathen et al, "Efficient continuous-wave four-wave mixing in bandgap-engineered AlGaAs waveguides," *Opt. Lett.* **39** 3161 (2014).
[12] K. Dolgaleva et al, "Compact ahighly-nonlinear AlGaAs waveguides for efficient wavelength conversion," *Opt. Express* **19** 12440 (2011).
[13] C. Lacava et al, "Nonlinear properties of AlGaAs waveguides in continuous wave operation regime" *Opt. Express* **22** 5291 (2014).
[14] H.C.H. Mulvad et al, "Demonstration of 5.1 Tbit/s data capacity on a single-wavelength channel. *Opt. Express* **18**, 1438 (2010).
[15] H. Hu et al, "Forward error correction supported 150 Gbit/s error-free wavelength conversion based on cross phase modulation in silicon," *Opt. Express* **21**, 3152 (2013).
[16] H.C.H. Mulvad et al, "Ultra-High-Speed Optical Serial-to-Parallel Data Conversion by Time-Domain Optical Fourier Transformation in a Silicon Nanowire," *Opt. Express*, **19** B825 (2011).